

Crystal chemistry and magnetic properties of ternary stannides R_2M_2Sn (R = rare earth or uranium, M = Ni, Pd)

B. Chevalier*, F. Fourgeot, D. Laffargue, P. Gravereau, L. Fournès, J. Etourneau

*Institut de Chimie de la Matière Condensée de Bordeaux, (ICMCB)-[UPR 9048], Université de Bordeaux I,
Avenue du Dr A. Schweitzer, 33608 Pessac, France*

Abstract

We have synthesized a great number of ternary stannides R_2Ni_2Sn , $R_2Pd_{2-x}Sn_{1+x}$ (R = rare earth) and U_2M_2Sn (M = Fe, Co, Ni, Ru, Rh, Pd, Ir, Pt). They crystallize either in the orthorhombic W_2CoB_2 -type or in the tetragonal U_3Si_2 -type. A structural relationship exists between these types and those of binary RNi and ternary $RNiSn$ or $RPdSn$ equiatomic compounds. Attention is also focused on the wide range of their magnetic properties [complex (B, T)-magnetic phase diagram, antiferromagnetic \Rightarrow ferromagnetic transition...]. © 1997 Elsevier Science S.A.

Keywords: Uranium; Rare earth; Stannides; Crystal structure; Magnetic properties

1. Introduction

The ternary uranium U_2M_2Sn stannides (M = Fe, Co, Ni, Ru, Rh, Pd, Ir, Pt) have been extensively investigated during the past 3 years due to their wide range of physical properties [1,2]. The existence of this family of uranium compounds allows us to study the influence of $5f(U)$ -ligand hybridization effects on the electronic and magnetic properties. These stannides except U_2Ir_2Sn and U_2Pt_2Sn crystallize in the tetragonal ordered version of the U_3Si_2 -type structure [3]. U_2Ir_2Sn and U_2Pt_2Sn adopt the tetragonal Zr_3Al_2 -type which is a superstructure of the U_3Si_2 -type [4].

Recently, some investigations have been carried out on some similar stannides based on cerium such as Ce_2Ni_2Sn [5,6] and $Ce_2Pd_{2-x}Sn_{1+x}$ [6-8]. Isotopic compounds can be obtained with other rare earth elements. A survey of their structural and magnetic properties is the subject of this present paper.

2. Results and discussion

All ternary stannides were prepared by melting of the constituent elements under a purified argon atmosphere. The samples were then annealed under vacuum at 800°C for 2-3 weeks. Their purity and chemical composition homogeneity were checked by microprobe analysis and X-ray powder diffraction.

2.1. Formation of the stannides

The ternary compounds R_2Ni_2Sn are obtained for R = Ce, Nd, Gd, Tb and Dy. Our attempts to synthesize Ho_2Ni_2Sn and Er_2Ni_2Sn have failed. Moreover the microprobe analysis performed on Tb_2Ni_2Sn and Dy_2Ni_2Sn samples reveals the presence of parasitic phases such as equiatomic stannide $TbNiSn$ or $DyNiSn$ and binary compound $TbNi_2$ or $DyNi_2$. It is certain that the stability of R_2Ni_2Sn stannides is governed by the size of the R-element.

Nowadays, the $R_2Pd_{2-x}Sn_{1+x}$ compounds can be obtained with R = Ce, Nd, Gd, Tb, Dy, Ho, Er and U

* Corresponding author.

and present a large range of homogeneity on the palladium rich side [6-10]. For instance these stannides exist with $R = \text{Ce}$ and U , respectively, for $0.04(3) \leq x \leq 0.21(4)$ [7] and $0 \leq x \leq 0.44(2)$ [9].

2.2. Crystal structure

All the $R_2\text{Ni}_2\text{Sn}$ compounds based on rare earths crystallize in the orthorhombic structure related to the W_2CoB_2 -type. R atoms form a three-dimensional network (Fig. 1) and constitute a $[\text{R}_8]$ prism surrounding either Sn atoms or Ni-Ni pairs. These last atoms are located inside a distorted $[\text{R}_6]$ trigonal prism. An interesting structural comparison concerns CeNi (CrB-type), $\text{Ce}_2\text{Ni}_2\text{Sn}$ and CeNiSn (TiNiSi-type) (Fig. 1) which contain trigonal prisms $[\text{NiCe}_6]$ more or less distorted. The formation of $\text{Ce}_2\text{Ni}_2\text{Sn}$ and CeNiSn

stannides arises from the insertion of Sn atoms into the $[\text{Ce}_6]$ prisms which are unoccupied in CeNi . According to the sequence $\text{Ce}_2\text{Ni}_2\text{Sn} \Rightarrow \text{CeNiSn}$, Sn fills a double $[\text{Ce}_6]$ prism so forming a $[\text{SnCe}_8]$ prism then a simple $[\text{SnCe}_6]$ trigonal prism.

The unit cell parameters of $R_2\text{Ni}_2\text{Sn}$ compounds decrease with the size of the rare earth (Table 1). This variation leads to a decrease of $d_{\text{Ni-Sn}}$ distance which varies from 0.2734(1) nm to 0.2642(1) nm following the sequence $\text{Ce}_2\text{Ni}_2\text{Sn} \Rightarrow \text{Dy}_2\text{Ni}_2\text{Sn}$. These values, much smaller than the metallic radii sum ($r_{\text{Ni}} + r_{\text{Sn}} = 0.2869$ nm), suggest a strong $3d(\text{Ni})-5p(\text{Sn})$ bond in these compounds.

All the $R_2\text{Pd}_{2+x}\text{Sn}_{1-x}$ compounds crystallize in the tetragonal $\text{Ce}_2\text{Pd}_{2+x}\text{Sn}_{1-x}$ -type structure (Fig. 1) where Pd excess atoms occupy one split position surrounding the replaced Sn atoms [7]. This structure is

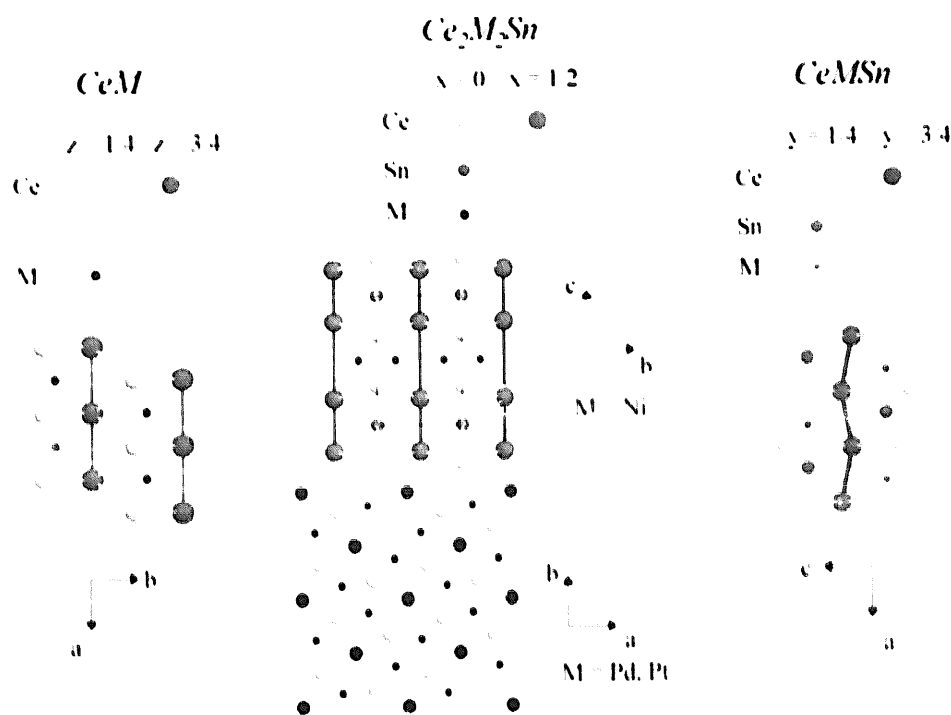


Fig. 1. Comparison of the crystal structure of CeM ($M = \text{Ni}$), $\text{Ce}_2\text{Ni}_2\text{Sn}$, $\text{Ce}_2\text{M}_2\text{Sn}$ ($M = \text{Pd, Pt}$) and CeMSn ($M = \text{Ni, Pd, Pt}$).

Table 1
Crystallographic data relative to $R_2\text{Ni}_2\text{Sn}$ stannides

R	Lattice parameters (nm)			Volume (nm ³)	Reference
	a	b	c		
Ce	0.4391(1)	0.5735(2)	0.8591(3)	0.2163	[6]
Ce	0.43936(9)	0.57396(9)	0.85967(13)	0.2168	[5]
Nd	0.4360(1)	0.5695(2)	0.8498(2)	0.2110	[11]
Gd	0.4294(1)	0.5638(1)	0.8390(1)	0.2031	[^a]
Tb	0.4278(1)	0.5614(1)	0.8332(1)	0.2001	[^a]
Dy	0.4247(1)	0.5615(1)	0.8273(1)	0.1973	[^a]

^a This work.

characterized by infinite columns of $[\text{Ce}_6]$ trigonal prisms surrounding Pd atoms and infinite columns of $[\text{Ce}_8]$ tetragonal prisms where Sn or Pd excess atoms take position.

2.3. Magnetic properties

Our recent investigations indicate that: (i) the magnetic properties of $\text{Ce}_2\text{Ni}_2\text{Sn}$ appear to be governed by a strong competition between the Kondo and RKKY magnetic interactions; it exhibits the behaviour of a magnetically ordered Kondo system having $T_K \cong 8$ K and $T_N = 4.7$ K, respectively, as Kondo and Néel temperatures [5]; (ii) at low fields, $\text{Nd}_2\text{Ni}_2\text{Sn}$ shows three ordering transitions, one antiferromagnetic occurring at 21 K and the others appearing, respectively, at 17.7 K and 14–15 K; the complex magnetic phase diagram of $\text{Nd}_2\text{Ni}_2\text{Sn}$ suggests a competition between the magnetocrystalline anisotropy produced by CEF effect and the oscillatory character of the RKKY exchange interactions [11].

As claimed previously, the purity of $\text{Tb}_2\text{Ni}_2\text{Sn}$ and $\text{Dy}_2\text{Ni}_2\text{Sn}$ samples is not good and their investigation by magnetization measurements confirm this statement. Three maximums are clearly visible on the $\text{Mag.} = f(T)$ curve concerning the temperature dependence of the magnetization of $\text{Tb}_2\text{Ni}_2\text{Sn}$ (Fig. 2): (i) the first appearing at 65(1) K could be attributed to the occurrence of antiferromagnetic ordering for this stannide; (ii) on the contrary, the others peaks around 42(1) K and 7(1) K, respectively, characterize the presence of TbNi_2 (ferromagnet at $T_f = 45$ K) [12] and TbNiSn (antiferromagnet at $T_N = 20$ K but exhibiting a canted structure at 7 K) [13]. The susceptibility of $\text{Tb}_2\text{Ni}_2\text{Sn}$ exhibits Curie-Weiss behaviour above 80 K; the parameters obtained by fitting are

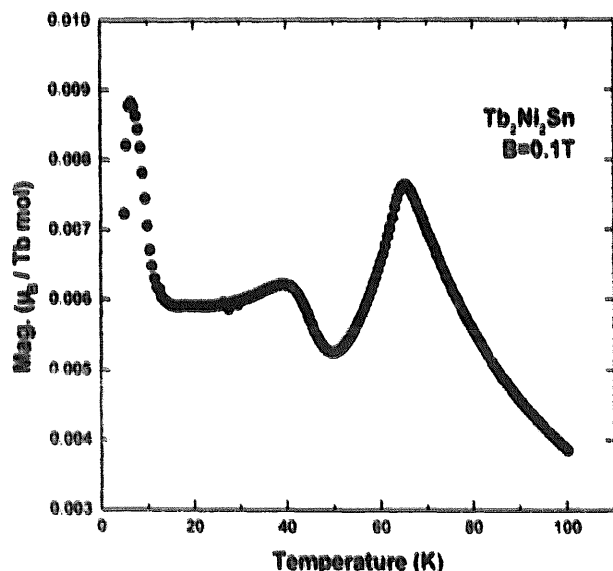


Fig. 2. Temperature dependence of the magnetization of $\text{Tb}_2\text{Ni}_2\text{Sn}$.

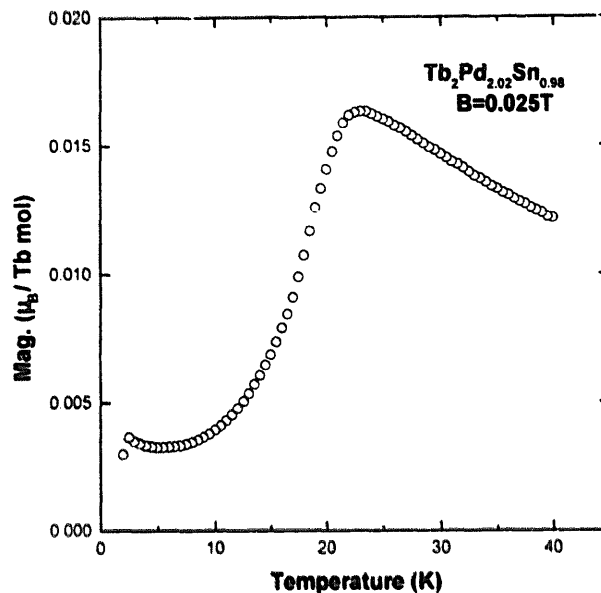


Fig. 3. Temperature dependence of the magnetization of $\text{Tb}_2\text{Pd}_{2.02}\text{Sn}_{0.98}$.

$\mu_{\text{eff}} = 10.23 \mu_B/\text{Tb}$ and $\theta_p = 39$ K. Neutron diffraction experiments are now in progress in order to establish the intrinsic magnetic properties of $\text{Tb}_2\text{Ni}_2\text{Sn}$.

Various magnetic properties are observed for $\text{R}_2\text{Pd}_{2-x}\text{Sn}_{1-x}$ stannides: (i) a phase transition between an incommensurate antiferromagnetic structure and a simple ferromagnetic one appears around 2.8–3.4 K for $\text{Ce}_2\text{Pd}_{2.04}\text{Sn}_{0.96}$ [14]; (ii) $\text{Nd}_2\text{Pd}_{2-x}\text{Sn}_{1-x}$ compounds order antiferromagnetically but the T_N temperature decreases with increasing x ($T_N = 8.8(3)$ K and 6.5(3) K, respectively, for $x = 0.02$ and 0.12). Moreover, these stannides exhibit several step-like field induced metamagnetic transitions [15]; (iii) neutron powder diffraction yields for $\text{U}_2\text{Pd}_{2-x}\text{Sn}_{1-x}$ non-collinear $k = (0, 0, 0)$ ($x = 0$) and collinear $k = (0, 0, 1/2)$ ($x = 0.35$) antiferromagnetic structures with magnetic moments at 1.5 K equal to 2.20(5) and 0.90(2) μ_B/U , respectively; the reduced U-magnetic moment observed for $x = 0.35$ can be correlated to an increase of the number of Pd atoms surrounding U ones and favouring the $5f(\text{U})$ – $4d(\text{Pd})$ hybridization [16].

All the $\text{R}_2\text{Pd}_{2-x}\text{Sn}_{1-x}$ stannides with $\text{R} = \text{Gd}, \text{Tb}, \text{Dy}, \text{Ho}$ and Er order antiferromagnetically. For instance, the magnetization of $\text{Tb}_2\text{Pd}_{2.02}\text{Sn}_{0.98}$ as a function of the temperature (Fig. 3) exhibits a maximum, indicating the onset of antiferromagnetic ordering at $T_N = 22(1)$ K. Also, at 2 K the field dependence of its magnetization evidences metamagnetic-like behaviour with a critical field of approx. 3.5 T. Similar measurements performed on $\text{R}_2\text{Pd}_{2.02}\text{Sn}_{0.98}$ compounds indicate that T_N is equal to 27.5(5), 13(1), 6(1) and 8(1) K for $\text{R} = \text{Gd}, \text{Dy}, \text{Ho}$ and Er , respectively.

References

- [1] F. Mirambet, B. Chevalier, L. Fournès, P. Gravereau, J. Etourneau, *J. Alloys Comp.* 203 (1994) 29.
- [2] M.N. Peron, Y. Kergadallan, J. Rebizant, et al., *J. Alloys Comp.* 201 (1993) 203.
- [3] F. Mirambet, P. Gravereau, B. Chevalier, L. Trut, J. Etourneau, *J. Alloys Comp.* 191 (1993) L1.
- [4] P. Gravereau, F. Mirambet, B. Chevalier, et al., *J. Mater. Chem.* 4 (1994) 1893.
- [5] F. Fourgeot, B. Chevalier, P. Gravereau, L. Fournès, J. Etourneau, *J. Alloys Comp.* 218 (1995) 90.
- [6] R.A. Gordon, Y. Ijiri, C.M. Spencer, F.J. DiSalvo, *J. Alloys Comp.* 224 (1995) 101.
- [7] F. Fourgeot, P. Gravereau, B. Chevalier, L. Fournès, J. Etourneau, *J. Alloys Comp.* 238 (1996) 102.
- [8] R.A. Gordon, F.J. DiSalvo, *J. Alloys Comp.* 238 (1996) 57.
- [9] F. Mirambet, L. Fournès, B. Chevalier, P. Gravereau, J. Etourneau, *J. Magn. Magn. Mater.* 138 (1994) 244.
- [10] F. Fourgeot, Thesis, University of Bordeaux I, 1576, 1996.
- [11] B. Chevalier, F. Fourgeot, L. Fournès, P. Gravereau, G. LeCaër, J. Etourneau, *Physica B* 226 (1996) 283.
- [12] J. Farrel, W.E. Wallace, *Inorg. Chem.* 5 (1966) 105.
- [13] J.K. Yakinthos, Ch. Routsis, *J. Magn. Magn. Mater.* 149 (1995) 273.
- [14] D. Laffargue, F. Fourgeot, F. Bourée, B. Chevalier, T. Roisnel, J. Etourneau, *Solid State Commun.* 100 (1996) 575.
- [15] F. Fourgeot, B. Chevalier, D. Laffargue, J. Etourneau, *J. Magn. Magn. Mater.* (to be published).
- [16] D. Laffargue, F. Bourée, B. Chevalier, T. Roisnel, P. Gravereau, J. Etourneau, *J. Magn. Magn. Mater.* 170 (1997) 155.